

Supplemental information

**Diversity and function of motile ciliated
cell types within ependymal lineages
of the zebrafish brain**

Percival P. D'Gama, Tao Qiu, Mehmet Ilyas Cosacak, Dheeraj Rayamajhi, Ahsen Konac, Jan Niklas Hansen, Christa Ringers, Francisca Acuña-Hinrichsen, Subhra P. Hui, Emilie W. Olstad, Yan Ling Chong, Charlton Kang An Lim, Astha Gupta, Chee Peng Ng, Benedikt S. Nilges, Nachiket D. Kashikar, Dagmar Wachten, David Liebl, Kazu Kikuchi, Caghan Kizil, Emre Yaksi, Sudipto Roy, and Nathalie Jurisch-Yaksi

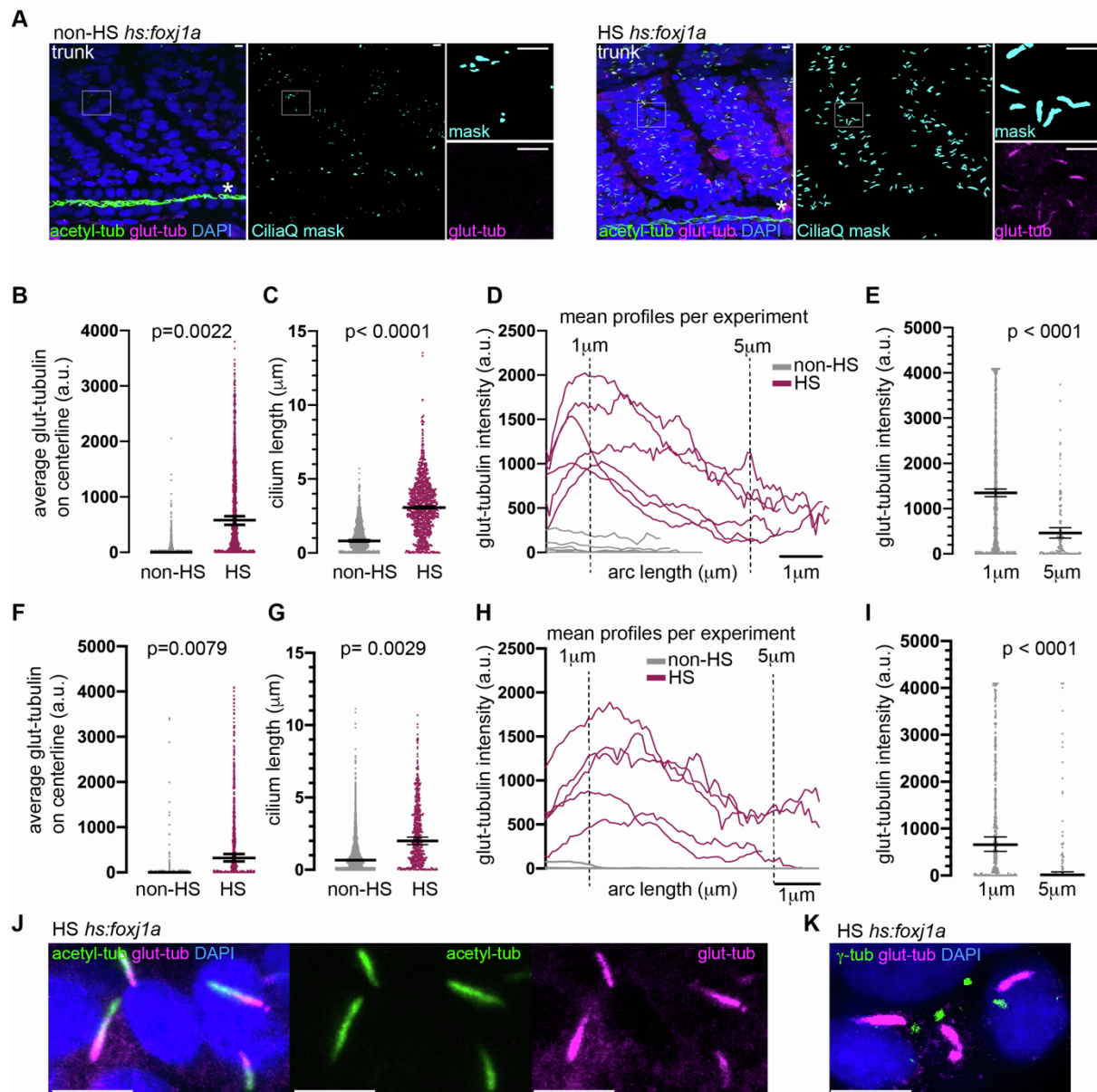


Figure S1. Glutamylated tubulin is enriched in cilia of foxj1-expressing cells. Related to Figure 1.

(A) Confocal image of the trunk of a control (non-HS, left) and heat-shocked (HS, right) *Tg(hs:foxj1a)* transgenic embryo at 24 hpf immunostained with acetylated tubulin (green), glutamylated tubulin (magenta) and DAPI. The acetylated tubulin signal was used for masking cilia using the CiliaQ software. Insets reveal longer and glutamylated-tubulin positive cilia in HS transgenic embryo as compared to non-HS control. Representative example of $n=6$. The pronephros, indicated with *, was excluded from the analysis.

(B, F) Overexpression of foxj1a by heat-shock increased tubulin glutamylation in cilia in the trunk (B) and eye region (F). Each dot represents an individual cilium collected from all images, bars: median \pm 95% confidence interval of median of all cilia. P-value by two-sided Mann-Whitney test on median of cilia from individual animals.

(C, G) Overexpression of foxj1a in HS animals increased cilium length in trunk (C) and eye region (G). Each dot represents an individual cilium, bars: median \pm 95% confidence interval of median of all cilia. p-value by unpaired, two-sided t-test with Welch correction on median of cilia from individual animals.

(D-E, H-I) The intensity of glutamylated tubulin staining is not uniform, but enriched at one end of the cilium in the trunk (D-E) and eye region (H-I).

(D, H) Each line represents the mean levels of glutamylated tubulin as a factor of position along the ciliary axoneme per embryo.

(E, I) Each dot represents the levels of glutamylated tubulin at 1 μm or 5 μm along the ciliary axoneme for all individual cilium, bars: median \pm 95% confidence interval of median. p with two-tailed Mann-Whitney test.

(J) Glutamylated tubulin (magenta) is enriched at one end of the cilium compared to acetylated tubulin (green), as shown in the representative confocal image of a 24 hpf HS *Tg(hs:fox1a)* embryo.

(K) Glutamylated tubulin (magenta) is enriched at the base of the cilium upon co-staining with the basal body marker gamma-tubulin (green), as shown in the representative confocal image of a 24 hpf HS *Tg(hs:fox1a)* embryo. Scale bars are 5 μm .

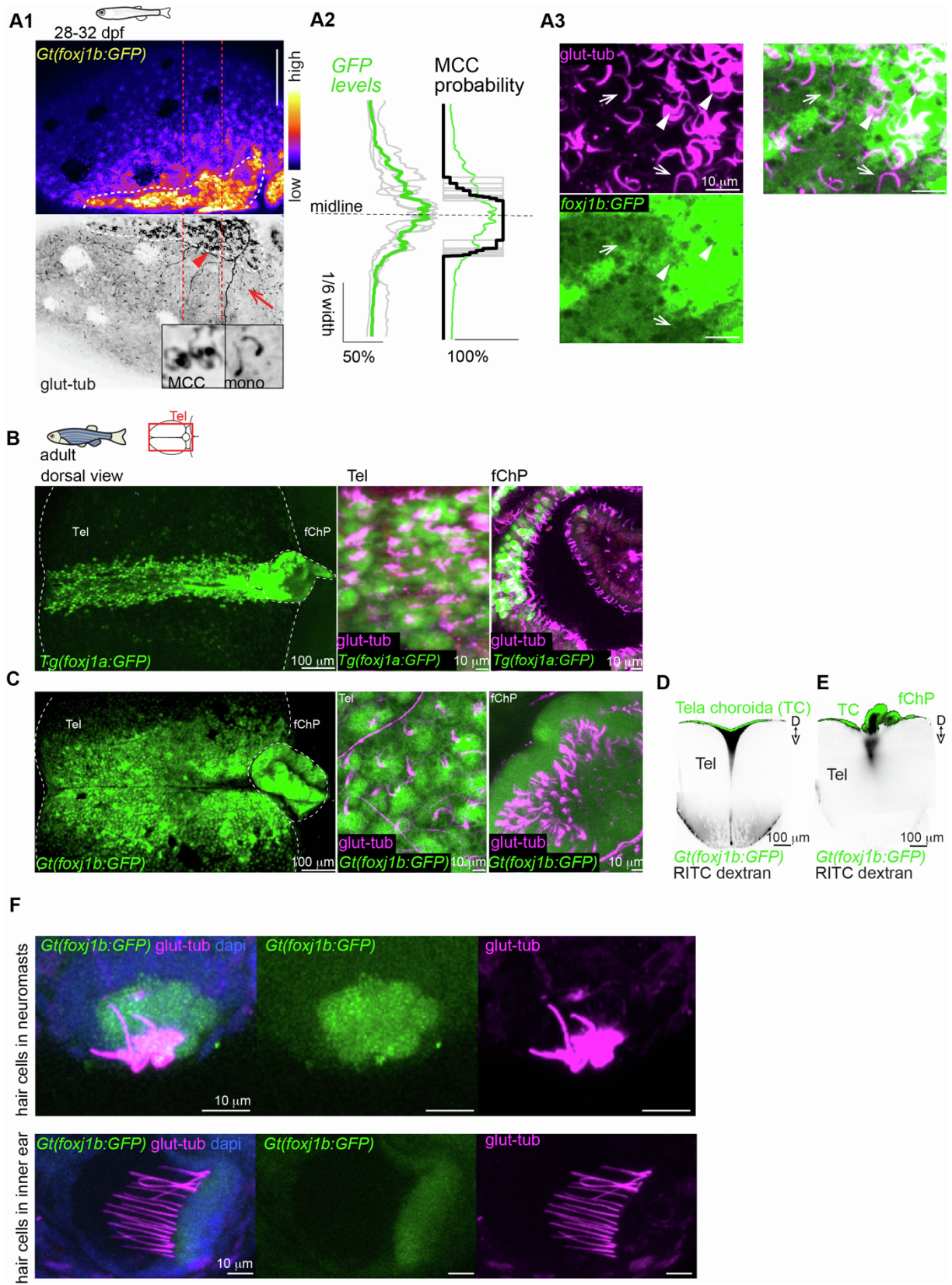


Figure S2. Ciliated cells located in the TC, telencephalon and ChP express *foxj1a*, *foxj1b* and *gmnc* to different extents. Related to Figure 3.

(A1-A3) At 28-32 dpf, *foxj1b* levels are correlated with multiciliation. **(A1)** *foxj1b:GFP* levels are higher in cells located in the medial part of the dorsal telencephalon (indicated with a dashed white line), which

is enriched in MCCs. The arrowhead shows a MCC and the arrow shows a monociliated cell, also magnified in the inset. **(A2)** Quantification showing higher GFP levels (relative GFP levels, n=6) and multiciliation (probability of n=9, as shown in Figure 1D3) in the 1 month medio-dorsal telencephalon (region indicated with a red line in panel C2). **(A3)** MCCs (arrowhead) express higher *foxj1b* than neighboring monociliated cells on the TC (arrow).

(B-C) In the adult brain, *foxj1a* and *foxj1b* are both expressed in the dorso-medial TC and ChP (n=3). Note that *foxj1a*-expressing cells **(B)** are located more medially than *foxj1b* **(C)** on the TC, and that only a subpopulation of ciliated cells express *foxj1a* in the ChP **(B)**. In contrast, all ciliated cells of the ChP express *foxj1b* **(C)**. *foxj1a:GFP* and *foxj1b:GFP* expressing cells bear glutamylated tubulin positive cilia (magenta).

(D-E) *foxj1b:GFP* expressing cells are in direct contact with CSF and are present **(D)** in the TC, which is the epithelial layer located above the CSF-filled cavity, and **(E)** in cells in the adult forebrain ChP surrounding CSF filled cavities, as shown upon injection of RITC-dextran (black) in a *Gt(foxj1b:GFP)^{tsu10Gt}* brain explant (n=3).

(F) Glutamylated tubulin is enriched in cilia of hair cells in neuromasts and inner ear as shown by confocal images of *Gt(foxj1b:GFP)^{tsu10Gt}* transgenic line immunostained for glutamylated tubulin (magenta) at 4 days (dapi in blue). Hair cells of neuromasts (top) and of inner ear (bottom) harbor glutamylated positive cilia.

D: dorsal, V: ventral, Tel: telencephalon, fChP: forebrain choroid plexus.

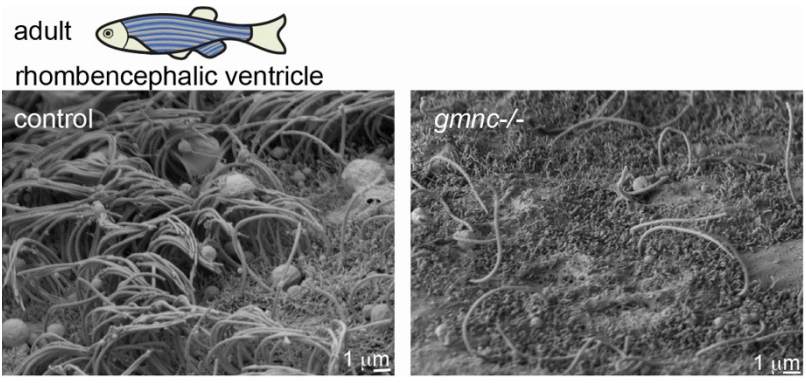


Figure S3: gmnc is required for multiciliation in ependymal cells in the rhombencephalic ventricle. Related to Figure 4.
Scanning electron microscopy images of the rhombencephalic ventricle (n=3).

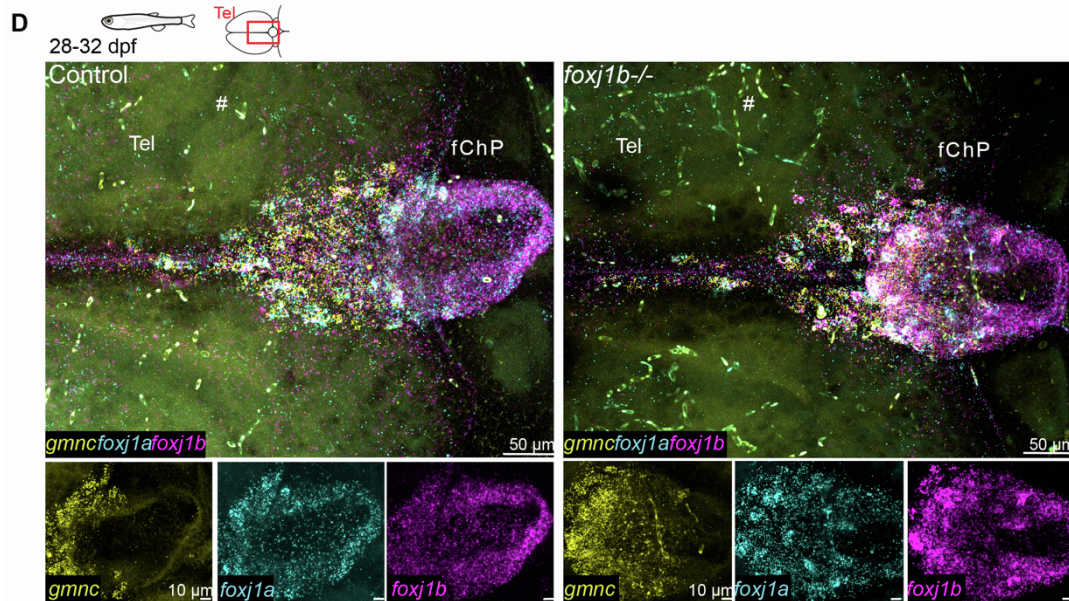
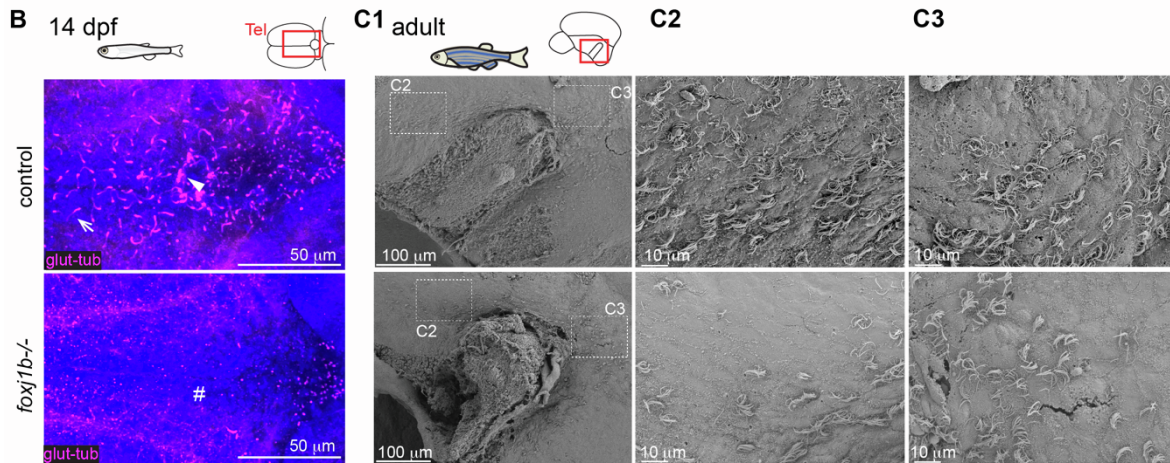
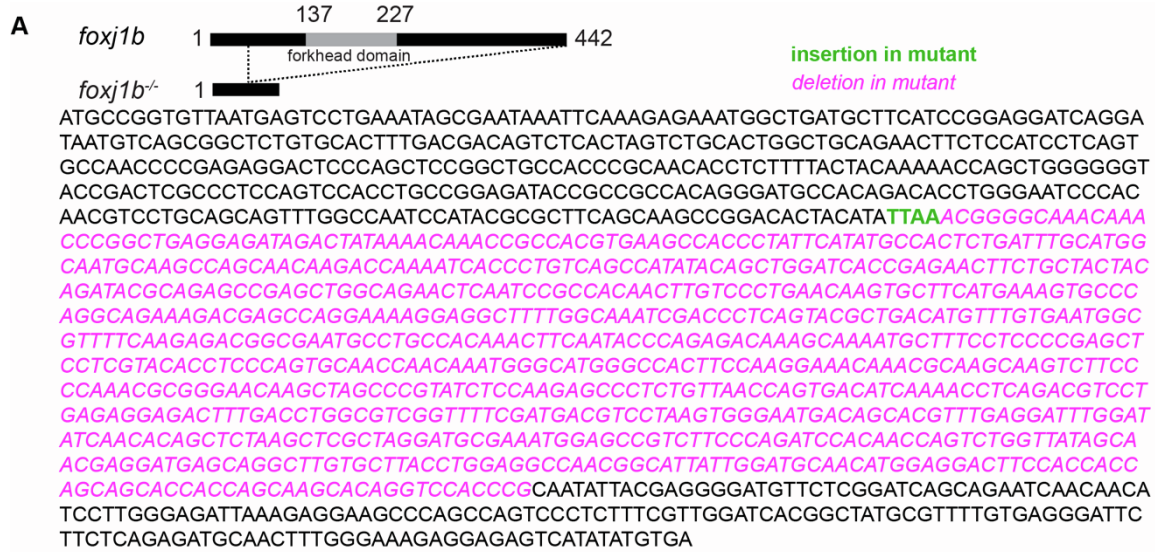


Figure S4. Schematic representation of the *foxj1b*^{sq5719} mutant allele and its ciliary defects. Related to Figure 5.

(A) A large part of the coding sequence of the *foxj1b* gene is lacking in the mutant allele, which includes the forkhead domain (grey). The allele contains a small insertion (indicated in bold green) and a large deletion (indicated in magenta red) of the gene.

(B) Confocal images at 2 weeks of age reveal that cilia are absent in the dorsal telencephalon of *foxj1b* mutant. Note the MCCs in the control (arrowhead). Cilia loss is indicated by #. (n=4).

(C1-C3) Ciliated cells remain in the midline of the telencephalon of *foxj1b* mutants as shown by SEM analysis (n=3). **(C2-C3)** Magnified insets as shown in C1.

(D) *foxj1b* does not influence *foxj1a* and *gmnc* levels in the TC and ChP as shown by multiplex HCR on 28 dpf control and *foxj1b* mutant animals. n=3 controls and 4 mutants.

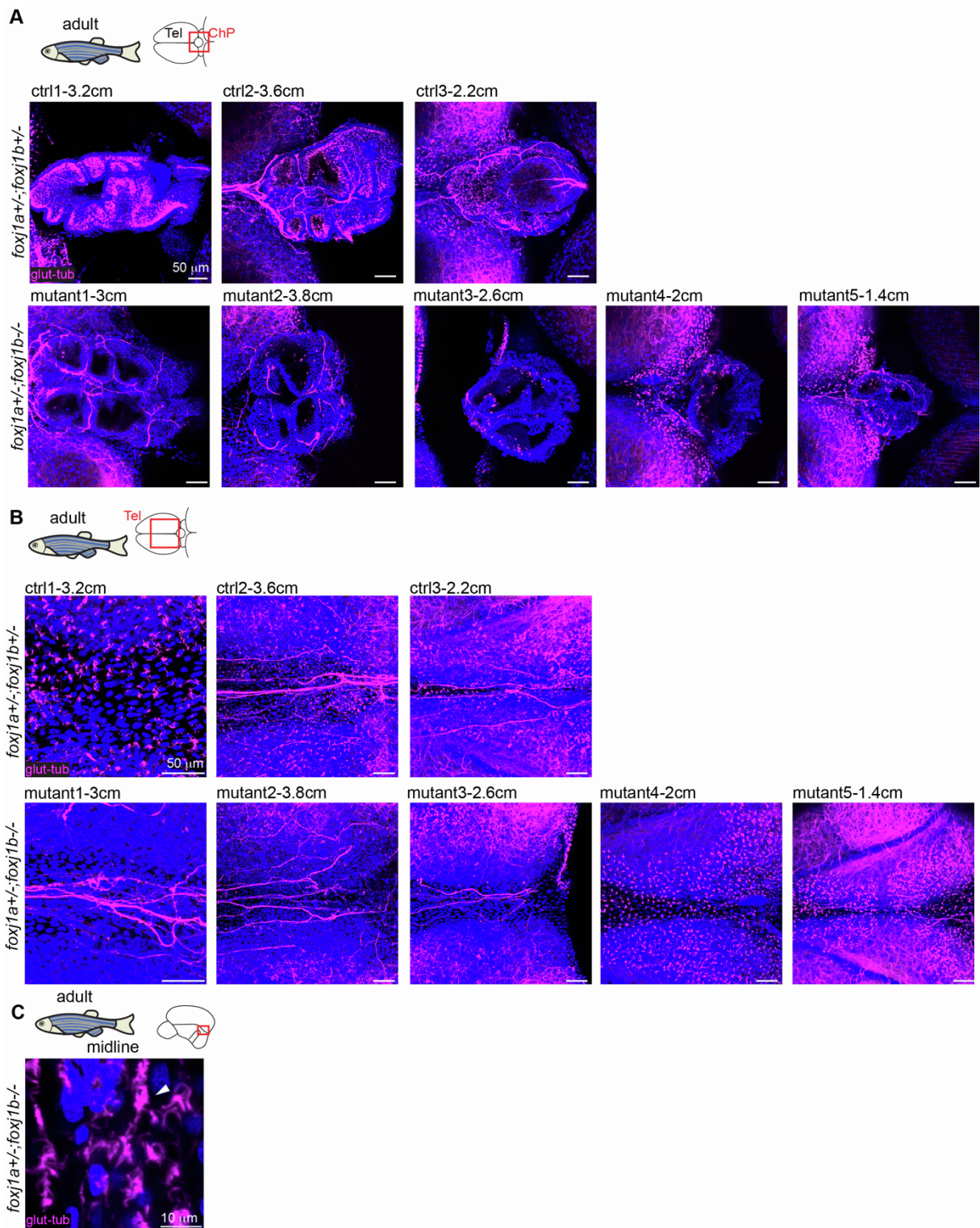


Figure S5. Ciliary defects in the brain of *foxj1a^{+/-};foxj1b^{-/-}* mutants are variable and more prominent in larger and older animals. Related to Figure 5

Confocal image of adult *foxj1a^{+/-};foxj1b^{+/-}* and *foxj1a^{+/-};foxj1b^{-/-}* immunostained for glutamylated tubulin (magenta) and DAPI (blue). **(A-B)** Partial loss of MCCs and total loss of single cilia in the ChP **(A)** and the medial TC **(B)** in *foxj1a^{+/-};foxj1b^{-/-}* as compared to *foxj1a^{+/-};foxj1b^{+/-}* controls. The effects are variable and more pronounced in larger/older animals. Body size (in cm) is indicated. **(C)** MCC remains in the telencephalic midline of *foxj1a^{+/-};foxj1b^{-/-}* (n=5)

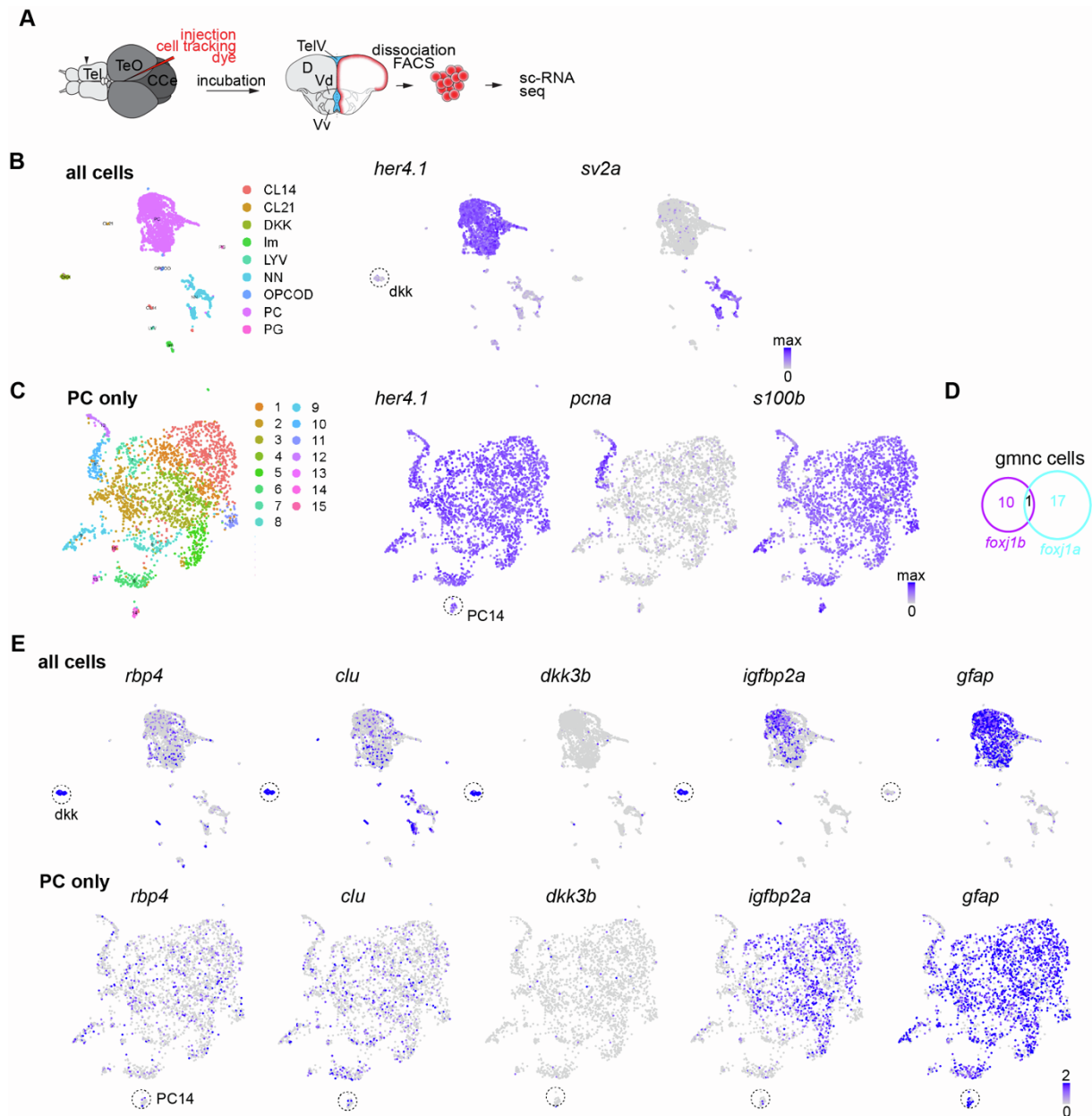


Figure S6. Diversity of motile ciliated cells in the adult telencephalon revealed by single cell RNA seq analysis. Related to Figure 6.

(A) Single cell transcriptomic analysis was performed on cells lining the telencephalic ventricle upon injection with a cell tracking dye. A total of 3158 cells were analysed.

(B) Unbiased clustering analysis of 3158 sequenced cells revealed the presence of 9 cell clusters expressing different cell markers, such as *her4.1* expressing progenitor cells (PC), *SV2a* expressing neurons (NN). Im: immune cells, LYV: *lyve1*-expressing cells, OPCOD: oligodendrocyte cells/progenitors, PG: pineal gland. Individual dots represented on these tSNE plots correspond to a single cell. Blue intensities indicate expression levels. Grey dots denote cells that do not express the specified gene.

(C) The progenitor cell cluster (PC) was re-clustered into 14 different clusters expressing *her4.1* broadly. A small percentage of cells expressed the proliferative marker *pcna* in contrast to the quiescent marker *s100b*.

(D) All cells with *gmnc* expression (total of 27) also expressed *foxj1a* and/or *foxj1b*.

(E) tSNE plots showing the expression of the genes differentially regulated between the *dkk* and PC14 ependymal clusters analysed by HCR.

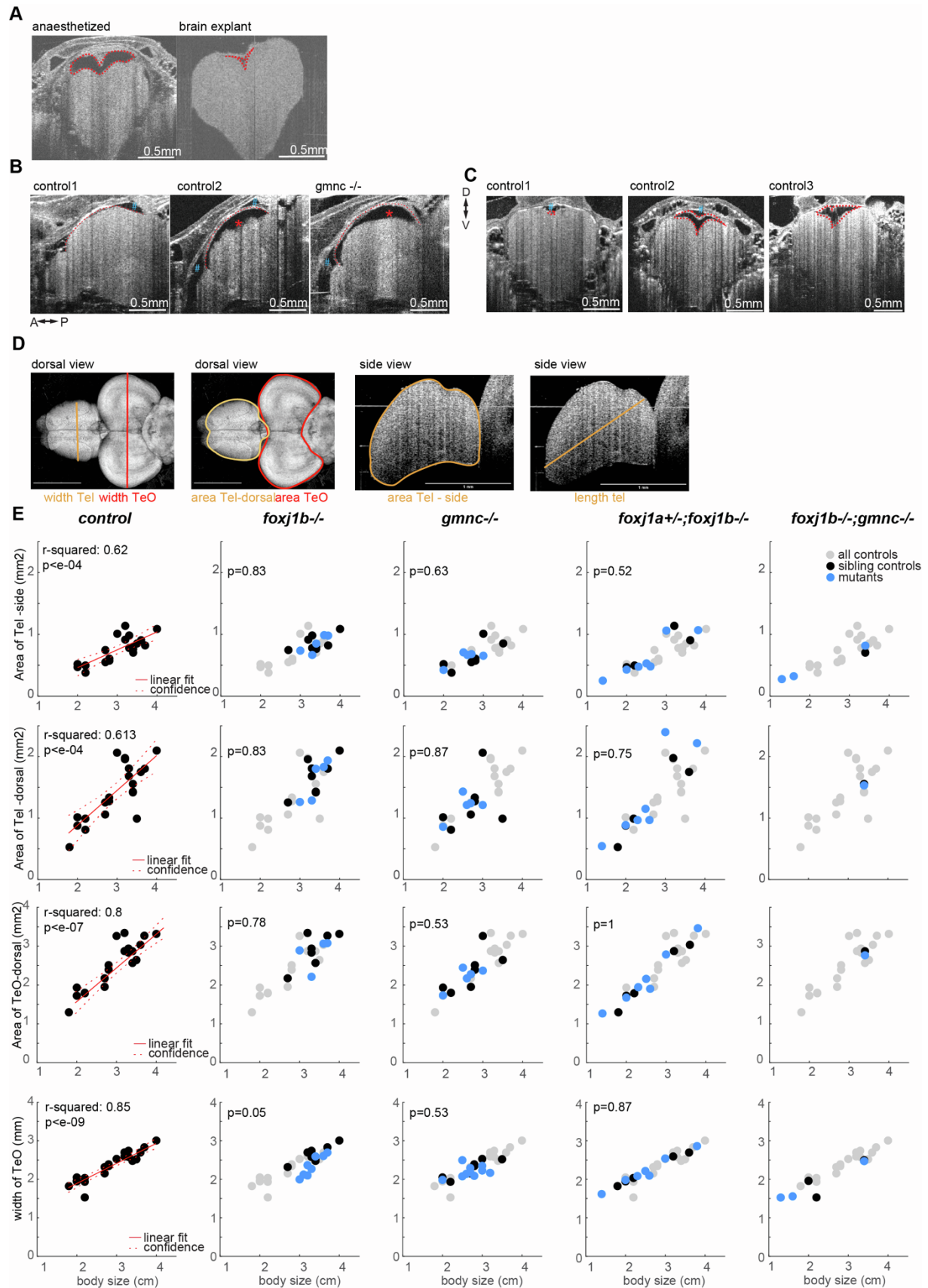


Figure S7. Imaging of brain ventricles and brain explants by OCT. Related to Figure 7.
(A) The telencephalic ventricle (indicated in red) collapses upon brain dissection.

(B) Fluid is present both within the ventricle (indicated with a red *) surrounded by the TC (indicated with a red dashed line), and within the skull (indicated with a blue #) outside the TC. Expansion of the telencephalic ventricle results in a reduction in volume of extra-ventricular liquid.

(C) Ventricles of control animals are of different sizes. Three examples are shown.

(D) Scheme indicating the different parameters quantified.

(E) Quantifications of brain sizes represented as a function of body length. Left: all controls pooled. The linear relationship between body size and the various parameters was calculated using a linear model fit and reported with r-squared and p-values. The linear fit is indicated in red with the confidence interval. Others: all controls in grey, sibling controls in black, mutants in blue. P-value (ranksum between sibling controls and mutants) are indicated in the graph. No p values are indicated for *foxj1b;gmnc* double mutants due to small sample size.

D: dorsal, V: ventral, A: anterior, P: posterior, TeO: optic tectum